MIDDLE EAST TECHNICAL UNIVERSITY

DEPARTMENT OF ELECTRICAL & ELECTRONICS ENGINEERING

EE 463- Static Power Conversion I

Wind Turbine Battery Charger

Hardware Project

Final Report

Prepared for Assoc. Prof. Ozan KEYSAN

DoesNotHertz

Birkan Genç- 2443059
Erdem Canaz - 2374676

Table of Contents

Introduction

As the energy industry moves to cleaner energy options, the significance of devices like DC-DC converters and rectifiers is rising, particularly with the growing use of renewable sources such as wind. This report delves into the design and implementation of a battery charger powered by a small wind turbine generator, highlighting the essential function of an AC-to-DC power converter circuit in managing variable input power. Through simulations and practical insights, the report addresses challenges, explores design parameters, and contributes to the development of sustainable energy systems.

Project Specifications

In this project we are aiming to design a battery charger. A small wind turbine generator will supply the variable input power. The primary challenge is to regulate the variable input power from the wind turbine, necessitating the development of an efficient AC-to-DC power converter circuit with control actions. The design will dynamically adjust the output current to adapt to the variations in input voltage caused by changing wind speeds.

Specifications of the system are listed below:

- **Input voltage:** 15 $V_{\text{line-line}}$ to 25 $V_{\text{line-line}}$
- **Battery capacity:** 100 Ah
- **Battery nominal voltage:** 12 V
- **Output current:** 10 A
- **Output current ripple:** 20% of average current

Design

a) Topology

Diode Rectifier & Buck Converter

We chose a 3-phase diode rectifier and buck converter topology to charge the battery because:

- Constructing a diode rectifier is relatively easy.
- Controlling the buck converter is straightforward due to its simplicity, involving only one switch that determines the output voltage value. This simplicity enables ease of control in the design of the battery charger, contributing to the overall efficiency and reliability of the system.

Given the project specifications, where a consistently higher input voltage than the battery voltage is required, the focus is on voltage reduction. The optimal solution lies in implementing a Buck converter. It's important to note that although the Buck converter excels in DC-to-DC conversion, the input source is three-phase AC. Consequently, integrating a rectifier circuitry becomes essential to have DC voltage at the output.

b) Units

The comprehensive system architecture is visually depicted in Figure 1 through block diagrams, with detailed explanations of the internal operations provided in subsequent subsections.

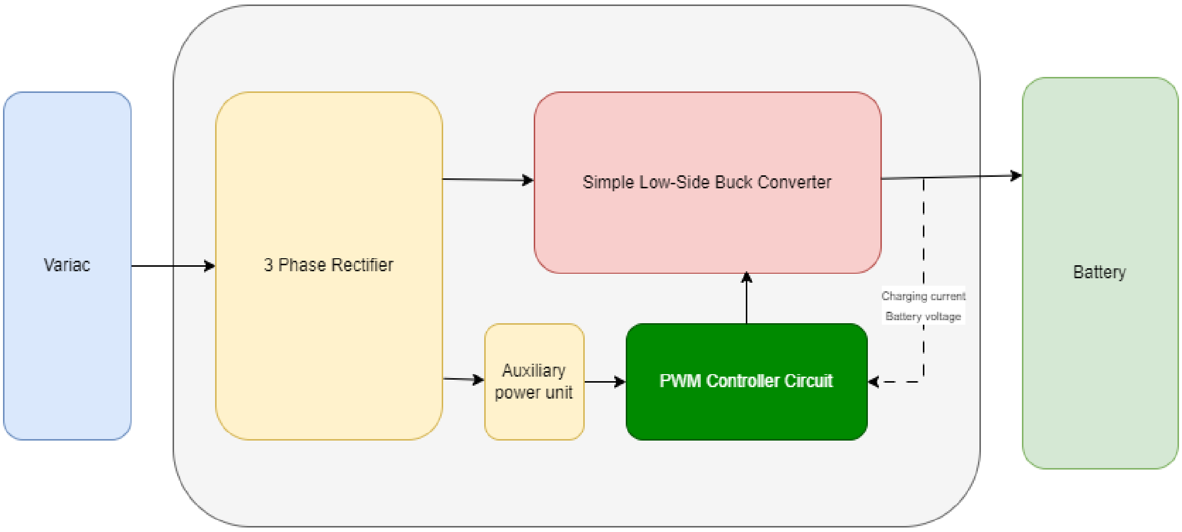

Figure 1. Simplified block diagram of the topology.

i) Three-Phase Full-Wave Diode Rectifier

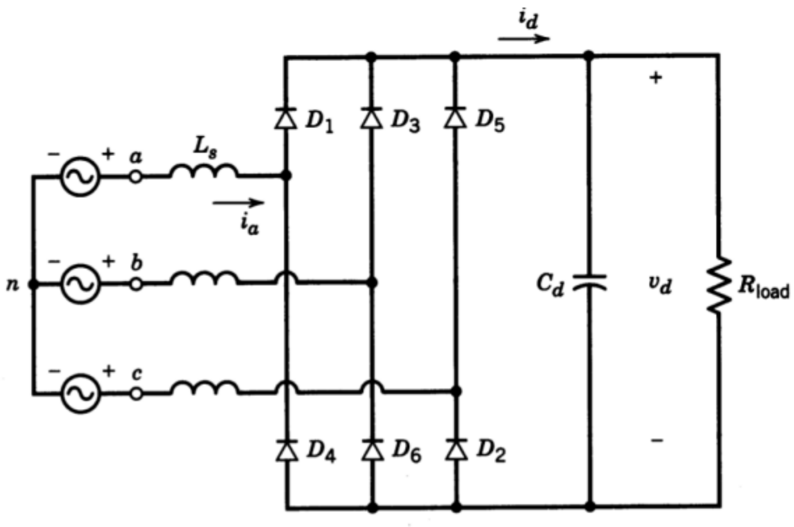

Figure 2. Three-phase full-wave rectifier circuit.

The voltage coming from the wind turbine will change between 15-25$V_{\text{line-line}}$. The voltage output formula of the three-phase full bridge rectifier is:

$$V_o = \frac{3\sqrt{2}}{\pi} V_{l-l} = 1.35 * V_{l-l}$$

$$minimum\ voltage\ at\ rectifier\ output \rightarrow 1.35 * 15 = 20.25$$

$$maximum\ voltage\ at\ rectifier\ output \rightarrow 1.35 * 25 = 33.75$$

As a result, the maximum and minimum output voltages will be between 20-35V. For the buck converter design, this voltage values must be considered.

ii) Low-Side Buck Converter

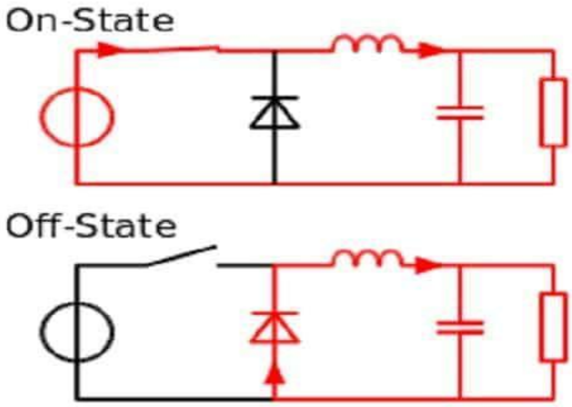

Figure 3. Basic buck converter circuit.

We prefer to utilize a MOSFET as the switch in the buck converter. The MOSFET's low ON-State Resistance ($R_{DS,on}$) minimizes conduction losses, and its low switching losses outperform those of other switching devices. Additionally, being voltage-driven devices, MOSFETs simplify the drive circuitry, contributing to an efficient design.

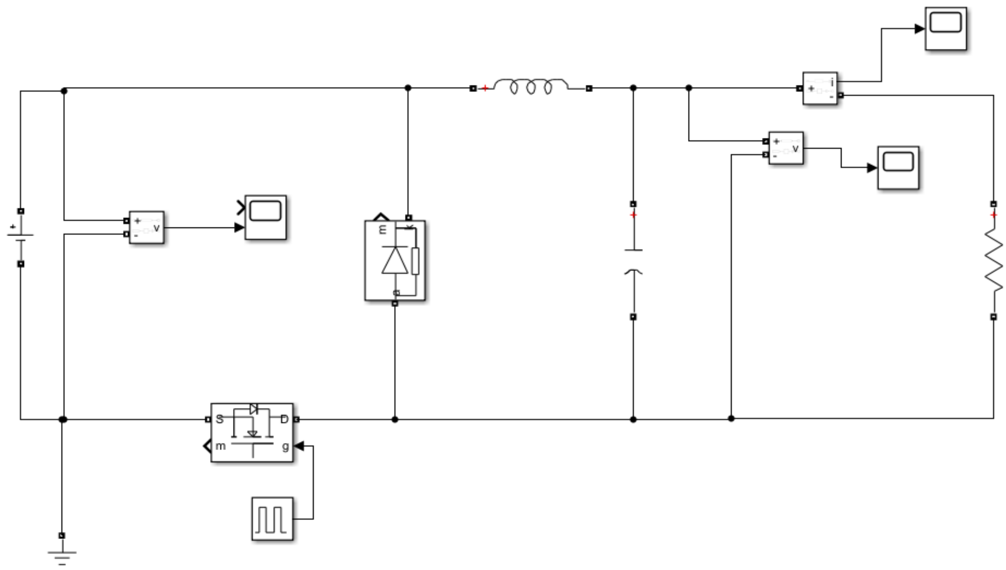

Figure 4. Low-side buck converter Simulink circuit.

In our battery charging unit design, we chose a low-side buck converter over a high-side buck converter. This choice allows us to use more readily available and cost-effective N-type MOSFETs than P-type MOSFETs. Although N-MOSFETs inherently can be driven directly by a PWM (Pulse Width Modulation) signal, our design incorporates a dedicated gate drive. This gate drive enables precise control over the N-MOSFET switching, ensuring optimal performance and efficiency in our low-side buck converter.

iii) Control Unit

For control, an Arduino Uno will serve as the digital controller in our design. The controller's task is to generate a PWM gate signal, controlling the opening and closing of the buck converter MOSFET. To maintain a constant charging current at 10A, the controller includes a current feedback loop from the buck converter output, adjusting the duty cycle accordingly.

Despite its relatively small power requirements compared to the charging power, ensuring the Arduino's stable operation is crucial. Hence, a 12V voltage regulator will be employed between the rectifier output and the Arduino to provide a reliable power supply and prevent unexpected circuit behaviours.

Electrical Calculations and Simulations

a) Buck Converter Inductance and Output Capacitance Calculations

The required current ripple is given as 20%. Since the output current is 10A, current ripple Δi_L is going to be 2A. We chose the switching frequency of the switch as 80 kHz. It is high enough so that we do not need to have a high inductance value.

For the inductance calculation, the worst-case scenario, which involves a high input voltage for the buck converter, specifically 35V, must be considered. So that the current ripple never exceeds 20%. Using the inductor equation below the minimum inductance value can be calculated.

$$D = \frac{V_o}{V_i} = \frac{12}{35} = 0.343, \qquad \Delta i_L = 2A, \qquad f_{sw} = 80\ kHz$$

$$\Delta i_L = \frac{(V_i - V_o)DT}{L}\ (switch\ on\ inductor\ charging)$$

$$L = \frac{(V_i - V_o)DT}{\Delta i_L} \rightarrow L = \frac{(35 - 12) * 0.343}{2 * 80000} = 49.3\ \mu H \tag{1}$$

As indicated in Equation 1, an inductance of 49.3 µH can be chosen to achieve a 20% current ripple. However, for enhanced stability, efficiency, and as a safety margin, we wanted to select an inductance in the range of 60-70 µH, ensuring lower current ripple and overall improved performance.

For the output capacitance calculations again, worst-case scenario will be considered. We want to have as low voltage ripple as possible, less than 2%. For calculation, the equation below can be used.

$$\Delta V_o = 12 * \frac{2}{100} = 0.24V$$

$$C = \frac{\Delta i_L T}{8 \Delta V_o} \rightarrow C = \frac{2}{8 * 0.24 * 80000} = 13\ \mu F \tag{2}$$

So, output capacitance can be chosen 13µF or higher.

b) Simulation Results with Calculated Values

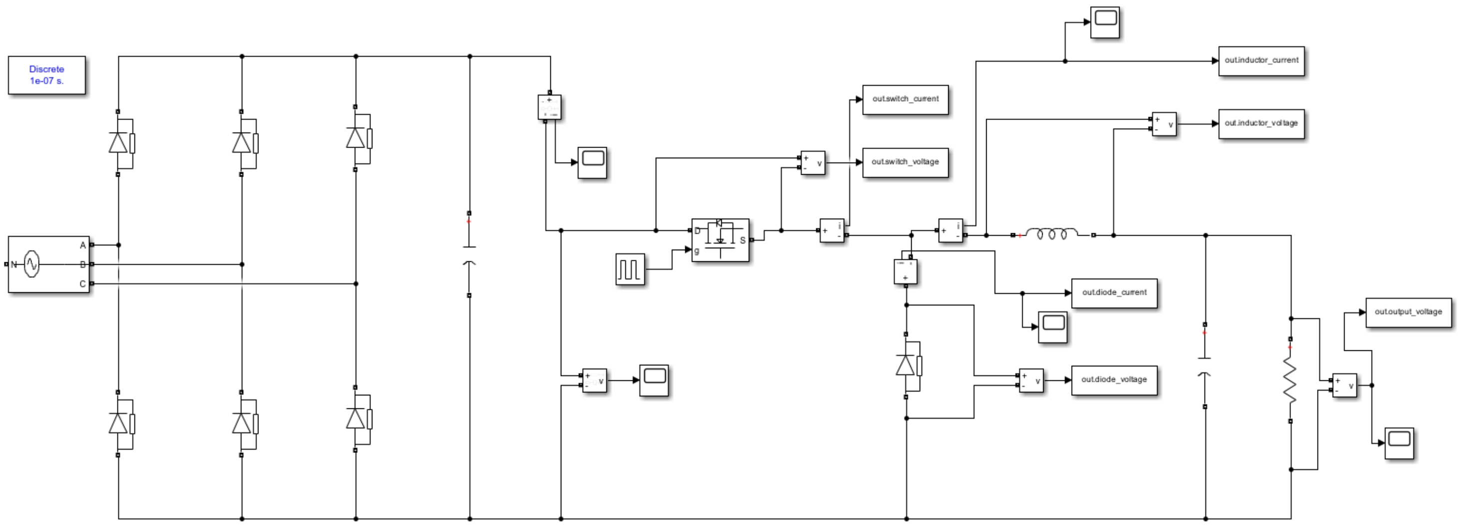

Figure 5. Simulink simulation circuit schematic.

The input AC voltage is given $25V_{l\text{-}l,\ rms}$ as it is the worst case. The duty cycle is set to 34% since the rectifier output is going to be around 35V. The load is 1.2Ω to have 10A current at 12V output. The simulation results are given below.

Rectifier

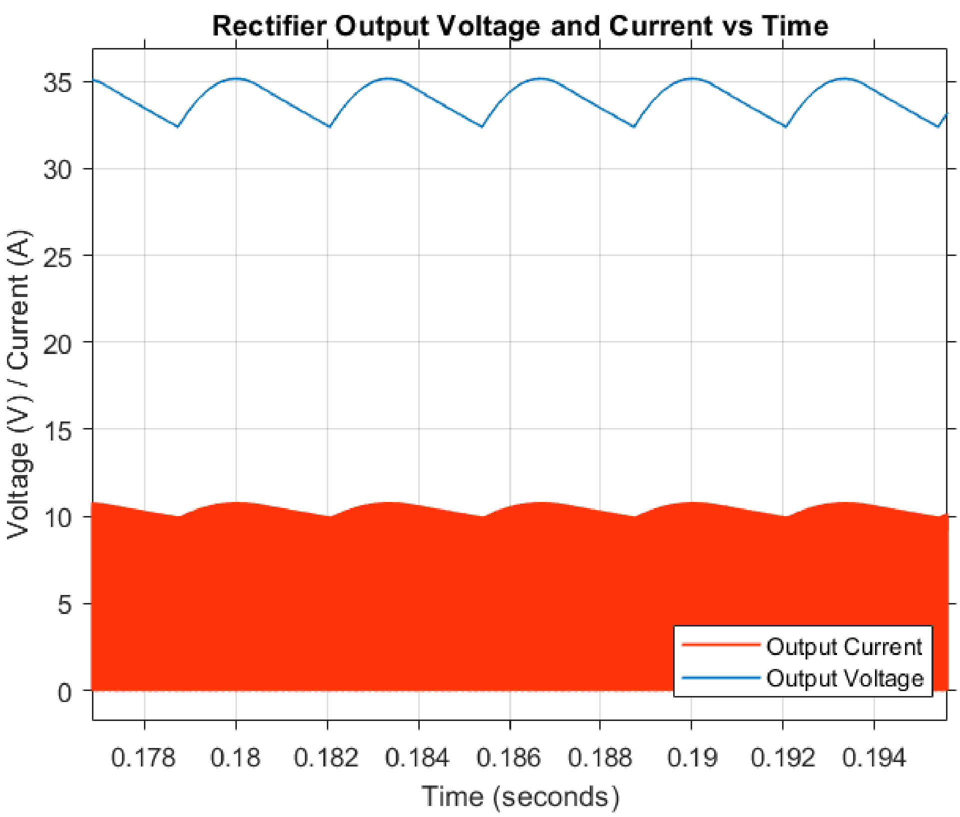

Figure 6. Rectifier Block Voltage and Current Output.

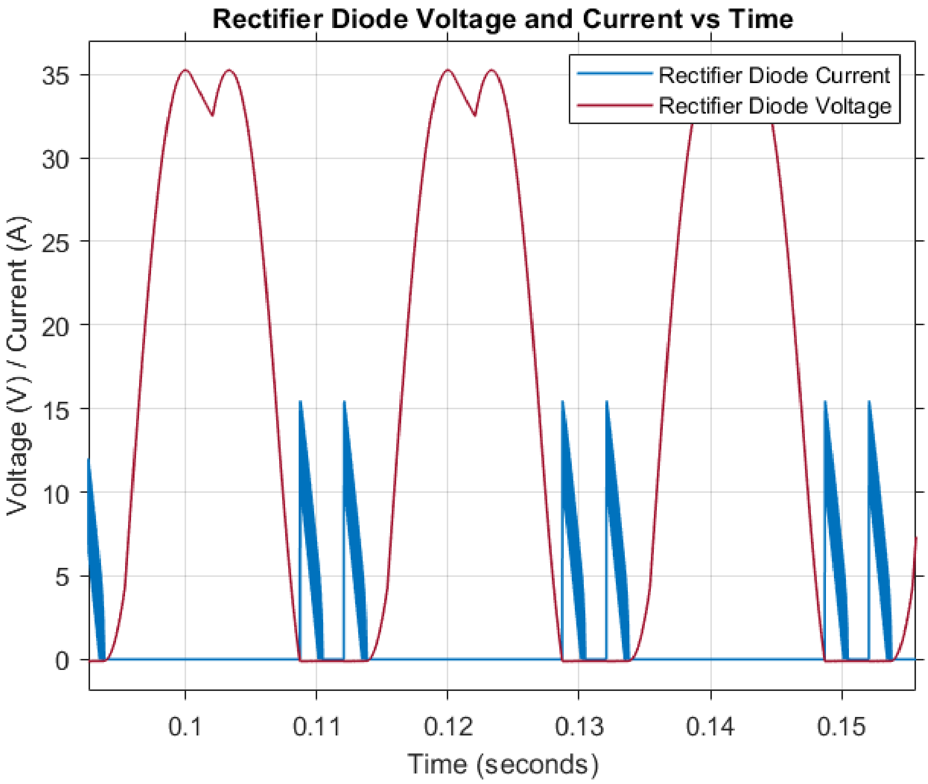

Figure 7. Rectifier diode voltage and current waveforms.

Buck Converter

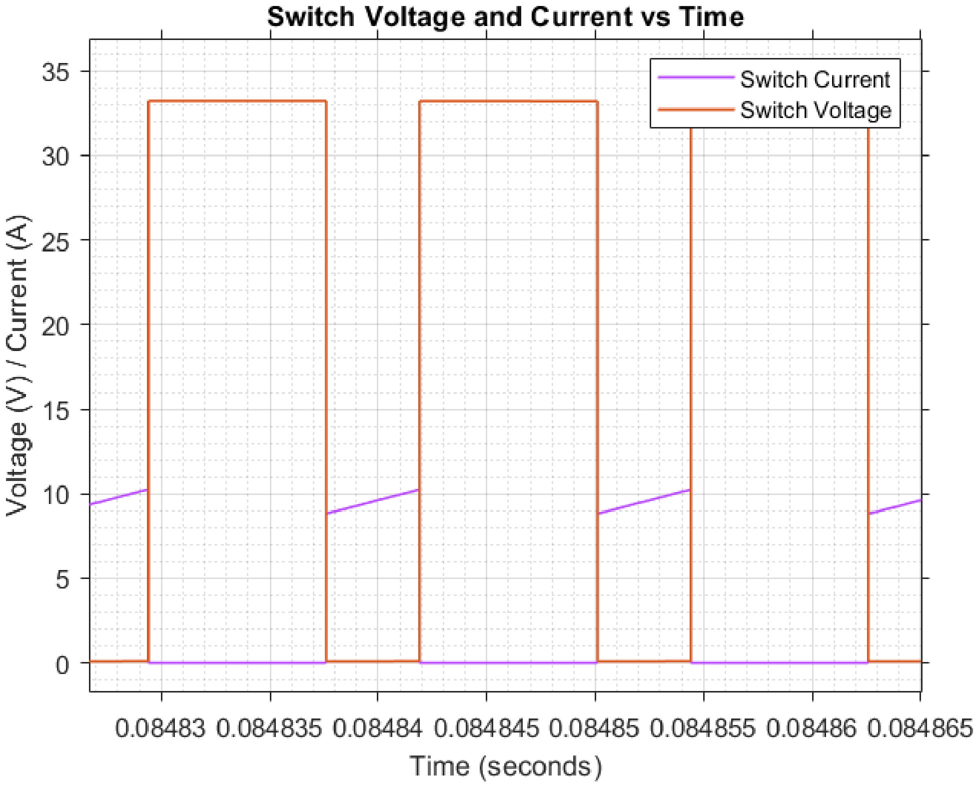

Figure 8. Switch voltage and current waveforms.

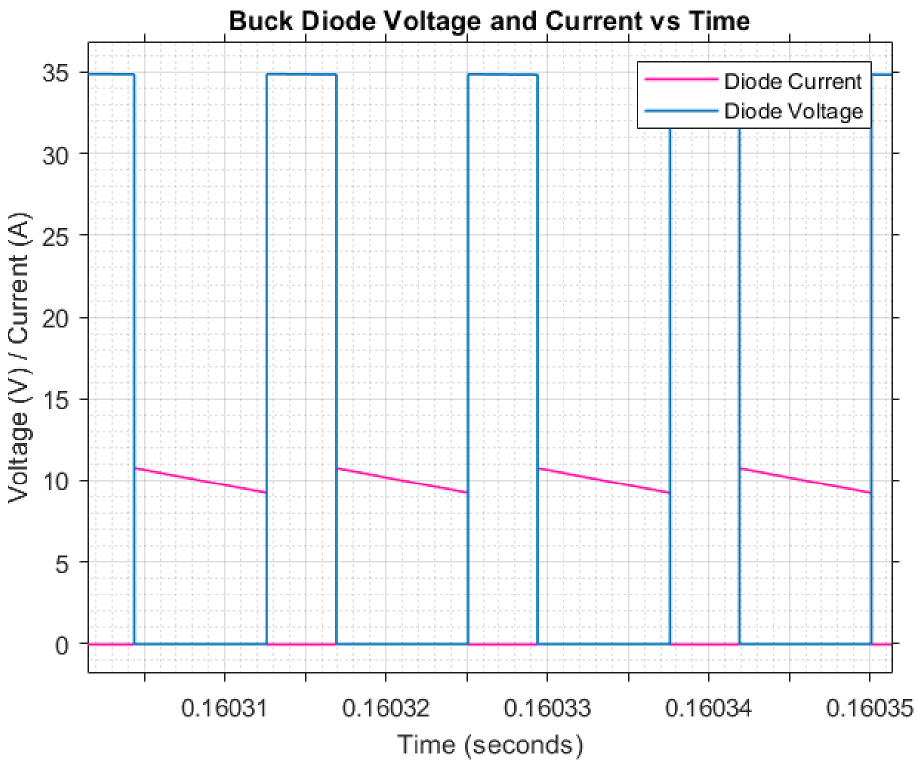

Figure 9. Buck converter diode voltage and current waveforms.

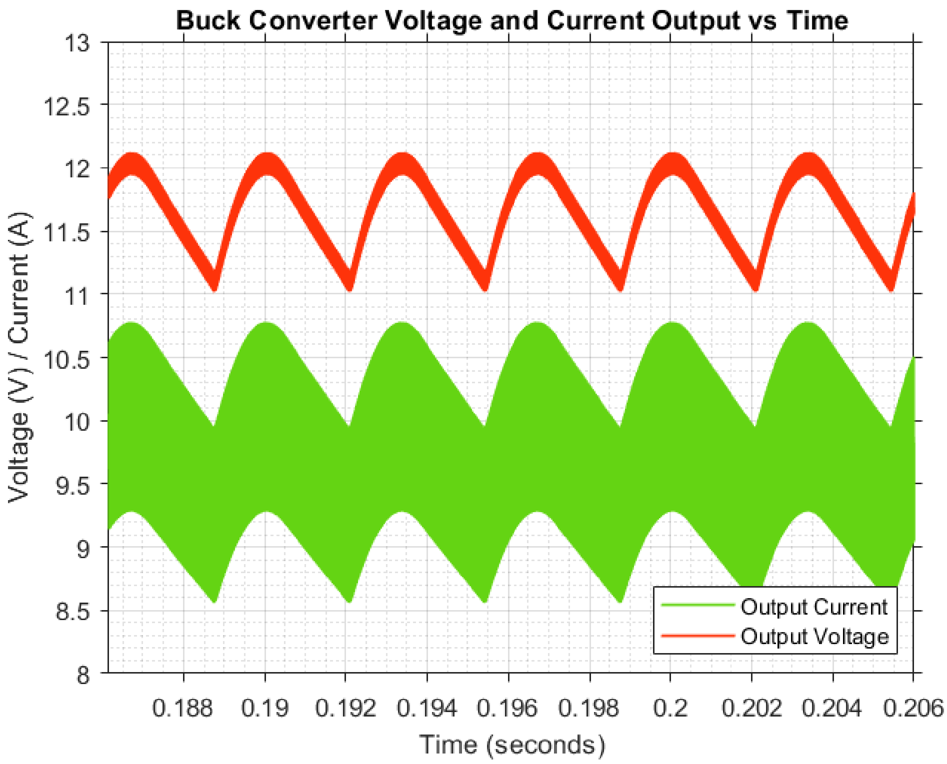

Figure 10. Buck converter output voltage and current waveforms.

The simulation results align with expectations; however, there is a slight elevation in the output current ripple compared to the anticipated values. Recognizing that the digital controller can influence current ripple by adjusting the duty cycle, we have decided to keep the calculated inductance value the same at approximately 65 µH. This choice allows for flexibility in controlling the current ripple through the digital controller while still meeting the overall design objectives.

Component Selection

The maximum voltage and current ratings for the components have been obtained from the preceding simulation section and will guide the appropriate selection of components. The corresponding values are detailed in Table 1 below.

Table 1. Maximum voltage and current ratings that obtained from simulation.

	Maximum Voltage	Maximum Current
Rectifier Diode	35 V	15 A
Buck MOSFET	33 V	11 A
Buck Diode	35 V	11 A
Rectifier Capacitor	35 V	-

Considering these values, along with an appropriate safety margin and aiming to minimize conduction and switching losses, our component selections are as follows.

Rectifier Diodes

MBR1560CT 60V 15A Schottky Diode (Datasheet)

RATED REPETITIVE REVERSE VOLTAGE	60V
AVERAGE RECTIFIED FORWARD CURRENT	15A
MAXIMUM REVERSE CURRENT	50mA
REVERSE RECOVERY TIME	50ns

MOSFET

IRFZ44 N Channel MOSFET 60V 50A (Datasheet)

COLLECTOR-EMITTER VOLTAGE	*60V*
GATE-SOURCE VOLTAGE	*+/- 20V*
COLLECTOR CURRENT	*48 A @ 25°*
POWER DISSIPATION	*110 W*
OPERATING TEMPERATURE	*-55°C / +175°C*

Buck Converter Diode

MBR1560CT 60V 15A Schottky Diode (Datasheet)

RATED REPETITIVE REVERSE VOLTAGE	60V
AVERAGE RECTIFIED FORWARD CURRENT	15A
MAXIMUM REVERSE CURRENT	50mA
REVERSE RECOVERY TIME	50ns

Capacitors

Rectifier Output capacitor: 2200 µF 50V

Buck Converter Output Capacitor: 22 µF 50V

Gate Driver

IR2102 MOSFET High and Low side driver (Datasheet)

MINIMUM PEAK OUTPUT CURRENT	210mA
VOLTAGE OUTPUT	10-20V
TEMPERATURE RANGE	150°C
MAXIMUM SWITCHING SPEED	160ns

Current Sensor

ACS712 Current Sensor 20A ([Datasheet])

Voltage Regulator

LM340T12 12V Voltage Regulator ([Datasheet])

Bill of Materials (BOM)

The costs of all circuit components used were checked on Digikey for a quantity of 1000 pieces.

Table 2. Unit price for 1000 pieces of each component used in the circuit.

Description	Component Name	Unit Price for 1000 pieces ($)
Rectifier Diode	MBR1560CT	0.73
2200 µF 50V Capacitor	-	0.64
22 µF 50V Capacitor	-	0.048
MOSFET Switch	IRFZ44EPBF	0.65
Buck Diode	MBR1560CT	0.73
Current Sensor	ACS712ELCTR-20A-T	1.83
Gate driver	IR2102	1.82
Digital Controller	Arduino Uno	27.6
12V Voltage Regulator	LM340T-12	1.11
Total:	35.158 $	

Thermal Calculations

In this section of the report, we will conduct a thermal analysis and assess the power losses associated with the semiconductor devices. The calculations are made considering the highest losses, maximum rated input voltage.

Conduction losses can be calculated using two methods, as outlined in Equation 3 and Equation 4. In the first method, the power dissipation can be determined by utilizing the forward voltage (V_f) drop of the semiconductor. Alternatively, the on-resistance (R_{ds}) value provided in the datasheet can be employed as another method for calculation.

$$P_{conduction} = V_f * I_{on} * D \tag{3}$$

$$P_{conduction} = R_{ds} * {I_{on}}^2 * D \tag{4}$$

Switching losses can be calculated, as demonstrated in Equation 5, by utilizing the turn-on energy (E_{on}) and turn-off (E_{off}) energy dissipated during the diode-switching process. In cases where these parameters are not provided in the datasheet, the switching loss can be estimated using the turn-on (t_{rise}) and turn-off (t_{fall}) delay times, as expressed in Equation 6.

$$P_{switching} = \left(E_{on} + E_{off}\right) * f_{sw} \tag{5}$$

$$P_{switching} \cong V_{off} * I_{on} * \left(t_{rise} + t_{fall}\right) * f_{sw} \tag{6}$$

MOSFET Losses

The MOSFET experiences an average current flow of 10A with a corresponding average voltage equal to the input voltage, which, in this case, is 35V. The R_{ds} value and other related values of the MOSFET can be found from the datasheet.

$$P_{MOSFET,cond} = 0.023 * 10^2 * 0.34 = 0.782\ W$$

$$P_{MOSFET,switch} \cong 35 * 10 * (60 * 10^{-9} + 70 * 10^{-9}) * 80000 = 3.64\ W$$

$$P_{MOSFET,total} = 4.422\ W$$

Diode Losses

Similarly, to the MOSFET, buck diode experiences an average current flow of 10A with a corresponding average voltage equal to 35V.

$$P_{diode,cond} = 0.65 * 10 * (1 - 0.34) = 4.29\ W$$

Heatsink Calculation

We want to operate maximum at 120 ºC. Thus, the required thermal resistance of the heatsink can be found using the equations below.

$$R_{CH}(Case\ to\ Heatsink), \qquad R_{JC}(Junction\ to\ Case), \qquad R_{HA}(Heatsink\ to\ Ambent)$$

$$T_{junc} = T_{ambient} + P_{loss}(R_{HA} + R_{CH} + R_{JC})$$

For MOSFET,

$$120 = 25 + 4.422 * (R_{HA} + 0.50 + 1.4)$$

$$R_{HA,needed} = 19.58\ °C/W$$

For diode,

$$120 = 25 + 4.29 * (R_{HA} + 3)$$

$$R_{HA,needed} = 19.14\ °C/W$$

In the implementation phase, we used two separate heatsinks that we already have for the diode and the MOSFET. The thermal resistances of the heatsinks were unknown. However, we did some testing with the thermal camera, and the temperature increase remained within our defined limitations. Consequently, we proceeded with the use of these heatsinks.

Gate Driver

We successfully implemented a gate driver, specifically the IR2102, for the buck converter. This was a crucial step, as the gate driver plays a pivotal role in power electronics, especially in handling the parasitic capacitances between the MOSFET's gate, source, and drain. These capacitances influence the switching behaviour, making it imperative to charge the gate capacitor quickly to turn the power device on and off efficiently. Our choice of the IR2102 allowed for effective control of these elements, ensuring a faster and more reliable switching process compared to direct control methods like using an Arduino. We configured the IR2102 for low-side switching, leaving the high-side pins unconnected. This setup was complemented by a 37-ohm resistor to connect the low-side output to the MOSFET gate, a decision guided by the need to limit the current to the highest rating of the driver, about 300mA. This precise configuration was essential because, as we learned, the output current from a logic IC or a PWM controller is typically insufficient for driving the gate of a power switch in high-power applications, often resulting in longer than desired switching periods.

Furthermore, we included safety measures like a 10k-ohm resistor between the gate and source pins of the MOSFET. This setup ensures an automatic shutdown of the MOSFET in case of a failure, a critical feature in power electronics where preventing damage due to faults is vital. Our design choices, particularly in selecting and configuring the gate driver, led to a substantial improvement in performance, reducing the MOSFET's turn-on time from around 600ns when switched directly with an Arduino to about 250ns, thus underscoring the effectiveness of using a dedicated gate driver. In addition to the previously mentioned components, we integrated bypass capacitors connected to the driver's power pins. This was a critical inclusion to counteract voltage drops across the parasitic feeder inductances, which can occur due to surge current demand. Specifically, we used one electrolytic and one ceramic capacitor to ensure the input voltage's stability further. The electrolytic capacitor provides bulk capacitance to absorb more significant, slower voltage fluctuations, while the ceramic capacitor deals with high-frequency noise, offering a fast response to sudden changes in current demand. This dual-capacitor strategy is essential in maintaining a stable voltage supply to the gate driver, thereby enhancing the reliability and efficiency of our buck converter design.

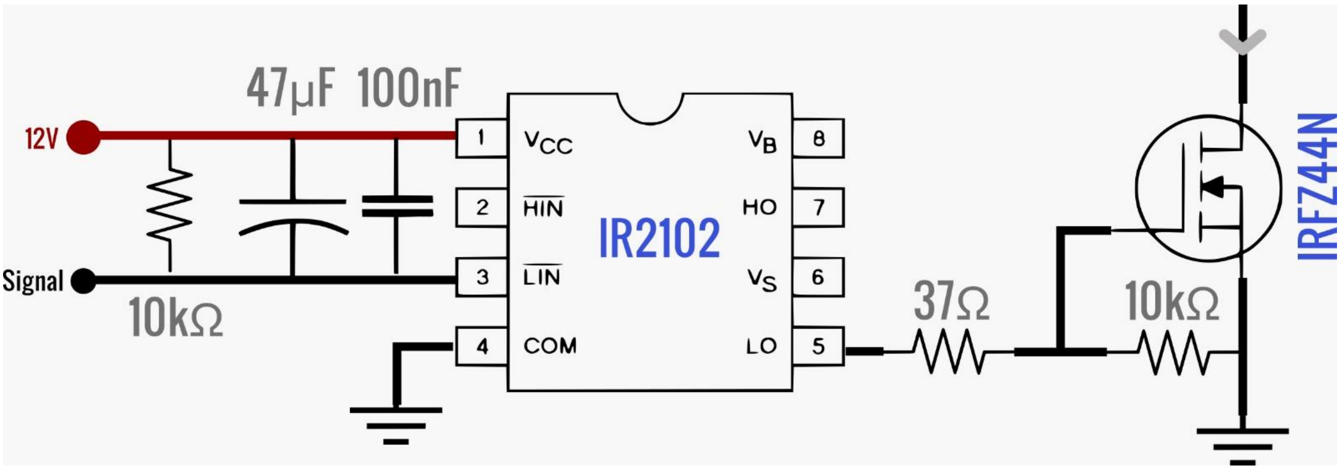

Figure 11. Gate driver circuit schematic.

Controller

We experimented with two methods to pursue effective charging current control. Initially, a digital controller acted as a proportional controller, adjusting the power gradually based on the desired current. While successful with a DC voltage source, it faced challenges with a variac due to the rapid voltage changes exceeding the controller's response speed. We considered increasing the output capacitor of the rectifier, which helps smooth out the current, but it was already large and didn't seem like a good solution. We then adopted a second method where the microcontroller reads the current and turns on or off the switch based on the desired current. Initially, we used analog reading, but it was too slow, causing issues like an increase of current up to 15A in just one decision cycle, as shown in Figure 12. Then we realized the importance of digitalizing the analog signal and implemented an opamp comparator circuit. It is known that Arduino's digital read takes around 5us, i.e., 80clock ticks. To make digital reading even faster, we used "Arduino port manipulation," which reads digital pins directly and very quickly, about 1MHz, while sacrificing the compatibility of the code with other Arduino devices. But then, the software's execution speed became the problem. We found it took about 6 microseconds for one cycle. Assuming the worst-case scenario with specific values (inductance of 75uH and a voltage of 28V), the ripple in the inductor was about 2.24A.

$$\Delta I = (6\mu s) \cdot \frac{28V}{75\mu H} = 2.24A$$

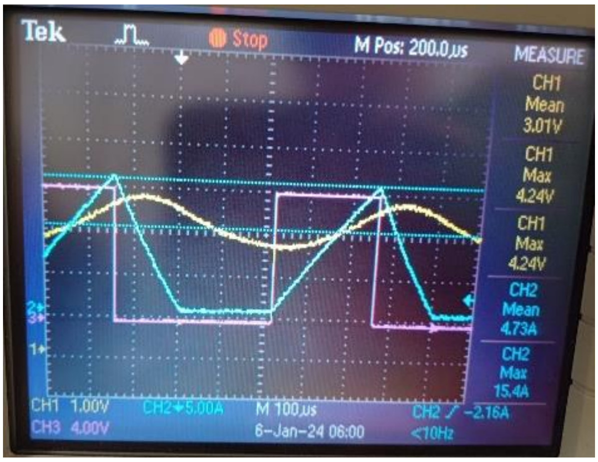

Figure 12. Analog read being slow for the 2. Method, where pink, blue and yellow waveforms represent gate signal, inductor current and analog current sensor output respectively.

Obviously, this ripple was handled mainly by the inductor and further smoothed out by the output capacitor, resulting in a nearly perfect DC current at the output. This is demonstrated in Figure 13.

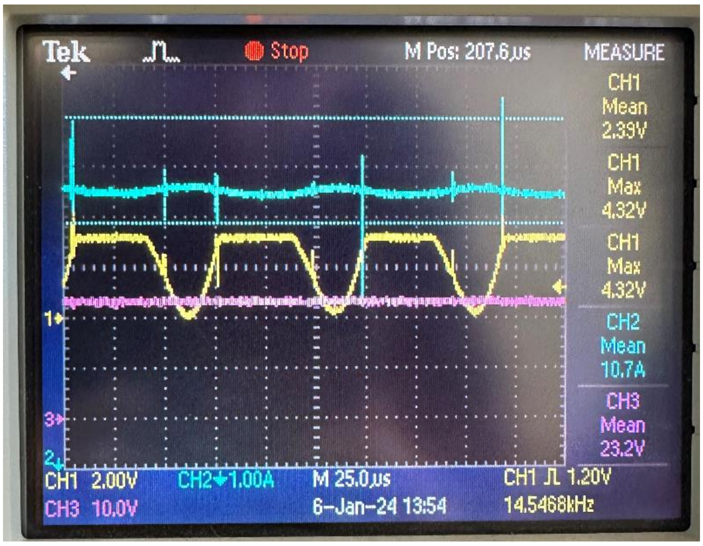

Figure 13. Measurements from demonstrated circuit where blue and yellow waveforms represents charging current and comparators' output respectively.

The simplified algorithm for the 2. Method can be seen in Fig. 14.

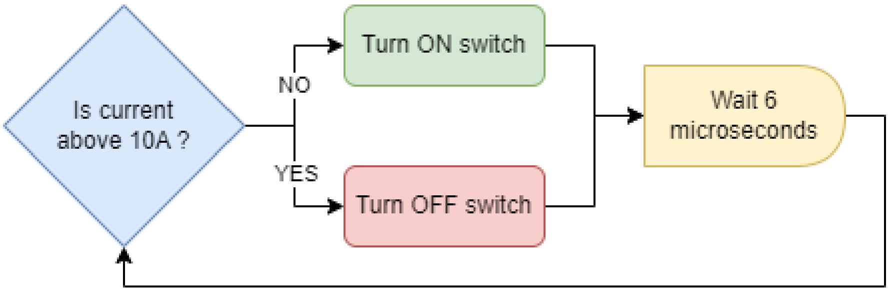

Figure 14. The simplified control algorithm for 2. Method.

Tests and Practical Results

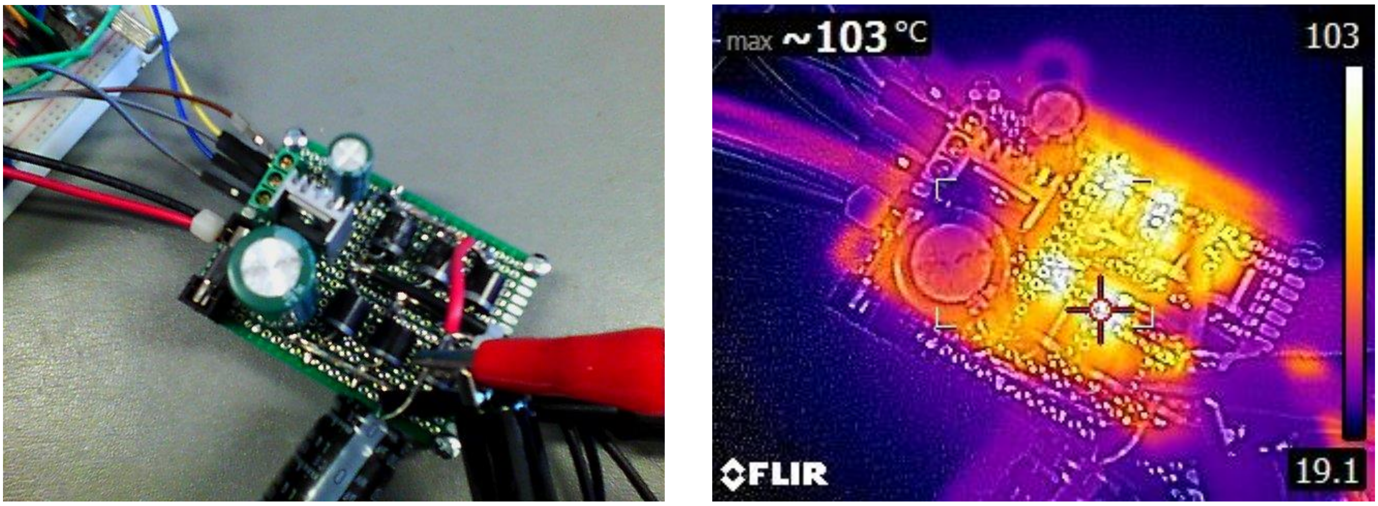

Figure 15. Thermal image of the rectifier block.

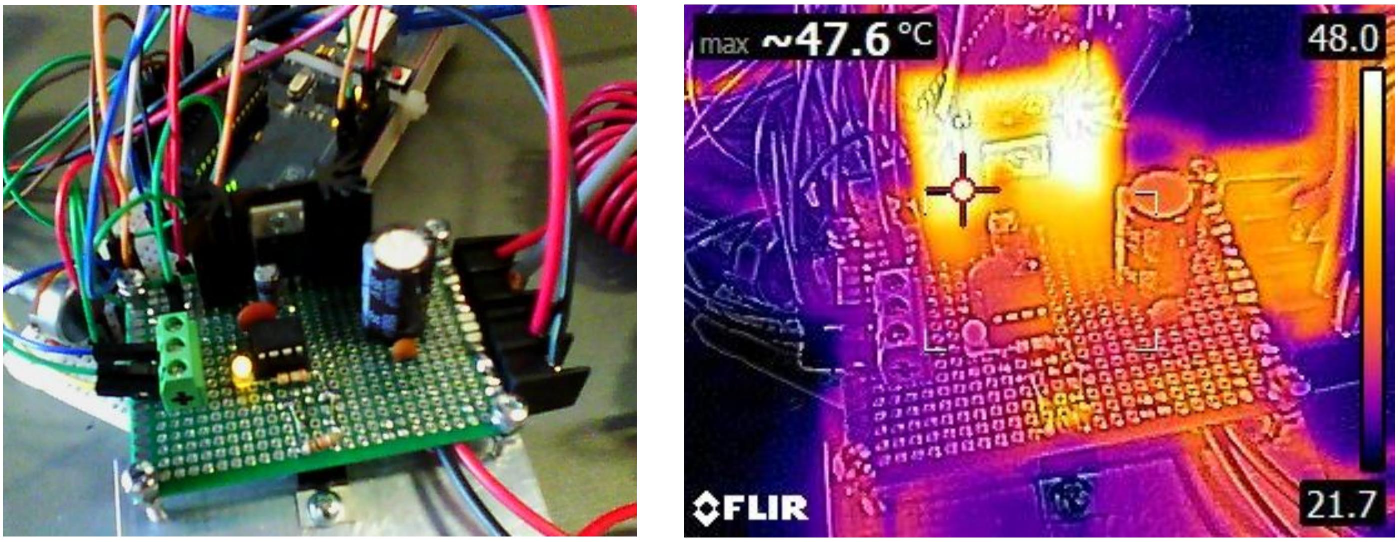

Figure 16. Thermal Image of the Buck converter block.

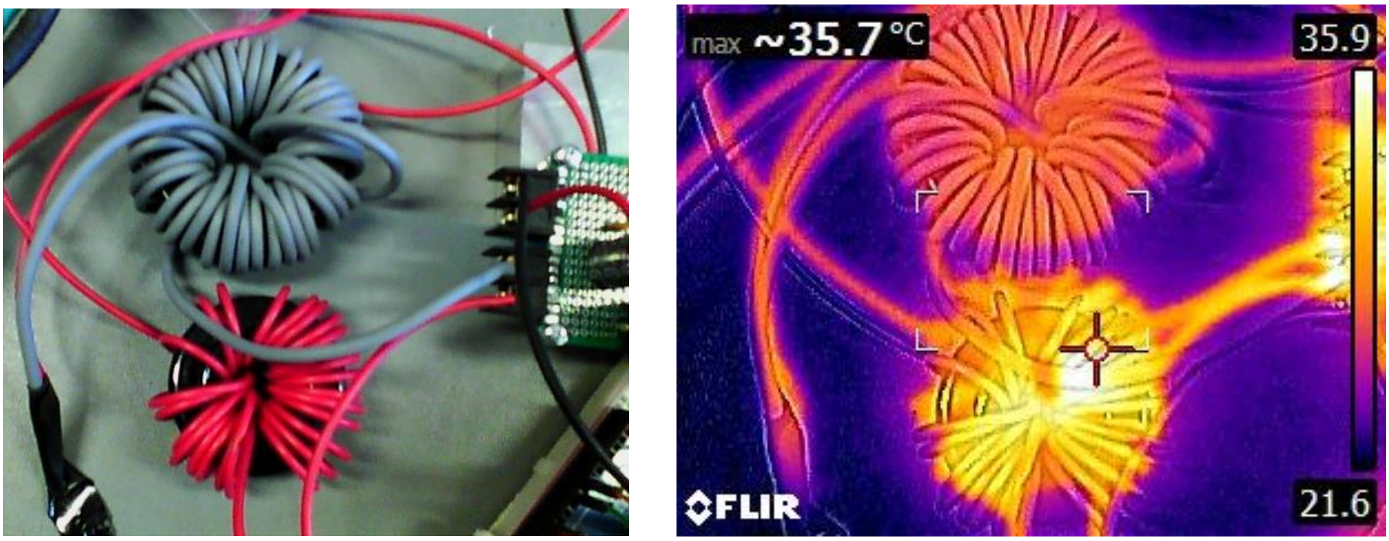

Figure 17. Thermal Image of the Inductors.

Figures 15, 16 and 17 show the temperature levels of several components after the circuit ran for a duration. All of the component temperatures were within the predetermined limits. However, the rectifier block was heating up faster than we expected. Implementing a heatsink or fan for cooling the rectifier diodes could have enhanced safety in this regard.

To eliminate the risk of core saturation, we chose two separate cores, connecting the inductors in series to achieve the specified inductance value in our design. While winding the inductances, we used cables of different diameters, with the grey cable having a larger diameter and the red cable having a smaller diameter. Figure 17 illustrates the impact of this choice, revealing that the smaller diameter cable, due to its higher resistance, dissipates more heat and consequently results in a greater increase in inductor temperature compared to the larger diameter cable.

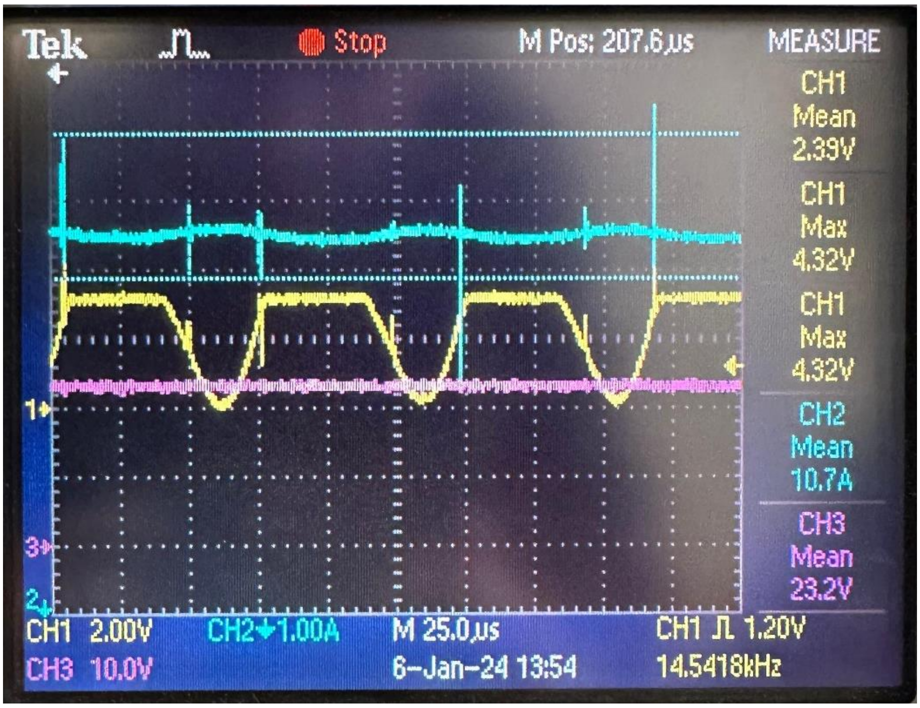

Figure 18. Buck converter input voltage, output current and feedback signals waveforms.

Figure 19. Buck converter input voltage, output current and feedback signals waveforms.

We connected the battery to our system and started to charge it. Figures 18 and 19 show the oscilloscope screens with changing input voltage. The purple voltage waveform represents the output from the rectifier, serving as the input to the buck converter. The yellow voltage waveform depicts the digital feedback signal coming from the comparator, while the blue current waveform represents the output current responsible for charging the battery.

The figures demonstrate the circuit's success in consistently maintaining the required current. The controller was responsive to the changes in the input voltage, quickly adjusting the duty cycle in case of voltage fluctuations and consistently keeping the output current around the anticipated 10 A level with low current ripple.

Conclusion

This project's primary objective was to design a battery charger driven by a small wind turbine generator, employing an AC-to-DC power converter circuit. The buck converter, serving as a crucial element, underwent simulations and subsequent modifications to optimize its performance. We decided to place the switch on the low side to simplify the gate topology and incorporated closed-loop feedback to ensure a precise current limit of 10A. The design extended to the implementation phase, where thermal calculations and board designs were crucial considerations. We tested our heatsink choices and the placements of the components. The circuit demonstrated its ability to maintain a consistent output current through practical testing with variable input voltages. This project has been an invaluable learning experience, providing insights into buck converter design, thermal design, gate drivers, and controller implementations, all contributing to a comprehensive understanding of power electronics applications.